

Energy dependence of ${}^9\text{Be} + {}^{12}\text{C}$ cross sections: Resonances or fluctuations

M. Hugi, J. Lang, R. Müller, J. Sromicki,* and E. Ungricht
*Laboratorium für Kernphysik, Eidgenössische Technische Hochschule, Hönggerberg,
8093 Zürich, Switzerland*

K. Bodek, L. Jarczyk, B. Kamys, A. Strzałkowski, and H. Witała
Institute of Physics, Jagellonian University, 30-059 Cracow, Poland

(Received 30 December 1981)

266 excitation curves for the emission of protons, deuterons, tritons, α particles, and ${}^8\text{Be}$ and ${}^9\text{Be}$ ions have been measured in the system ${}^9\text{Be} + {}^{12}\text{C}$. Data were taken in 107 keV steps in the energy range from 5.9 to 15.4 MeV (c.m.) at several angles between 5° and 175° (lab). The results were analyzed on the basis of the statistical reaction model and various statistical methods for localizing possible correlated structures were used. The fluctuations are shown to be in agreement with the predictions of the statistical model and no marked correlations between different channels were found.

NUCLEAR REACTIONS ${}^{12}\text{C}({}^9\text{Be},x)$, $x = p, d, t, \alpha$, ${}^8\text{Be}$, and ${}^9\text{Be}$; measured $\sigma(E_x, \theta_x)$, $E_{\text{c.m.}} = 5.9 - 15.4$ MeV. Statistical analysis of excitation curves; unsuccessful search for resonances.

I. INTRODUCTION

In recent years, experimentalists were inspired in their search for molecular resonances in heavy ion systems by a paper of Hanson *et al.*,¹ who indicated those systems as especially favorable which are characterized by a low level density *and* by a small number of open channels. In a compilation listed in this paper, the system ${}^9\text{Be} + {}^{12}\text{C}$ was placed among the most promising ones. However, the attempts to find such resonances in the energy region from 2.40 to 6.43 MeV (c.m.), reported in the same paper, were unsuccessful. Although several publications²⁻⁵ concerning possible resonances have appeared since that time, the situation is still far from a satisfactory solution. This could be connected with some special properties of the ${}^9\text{Be} + {}^{12}\text{C}$ system: Firstly, the channel spin in the entrance channel is different from zero ($\frac{3}{2}$). Secondly, owing to the low binding energy of ${}^9\text{Be}$, direct reaction processes play a significant role already at low energies, not far above the Coulomb barrier. As shown in an experiment in which the fusion cross section was determined from the emission of light particles, the compound nucleus formation covers only about 70% of the total reaction cross section.⁶ The remaining 30% appear as direct reaction contributions in several reaction channels, mainly in reac-

tions with α particle or ${}^8\text{Be}$ emission and in elastic and inelastic scattering. Such a large direct reaction component in the cross section enhances the absolute magnitude of the fluctuations in the excitation curves.⁷ Therefore, possible real resonances might be obscured or, on the other hand, some large fluctuations could be confused with resonances.

The present experiment was undertaken in order to provide a comprehensive set of excitation curves for a search for resonances. A lot of reaction channels have been measured in a broad energy region and at many angles both in the forward and in the backward hemispheres. Preliminary results have already been published.³ No clear evidence of any correlated structures followed from this work. The present paper contains the results from measurements of excitation curves for the emission of protons, deuterons, tritons, α particles, and ${}^8\text{Be}$ nuclei to different final states of the residual nuclei as well as for elastic scattering. The data were taken in steps of 107 keV in the energy range from 5.9 to 15.4 MeV (c.m.) at many different angles between 5° and 175° (laboratory).

The statistical character of the obtained results was checked in an extended analysis based on the statistical reaction model. This analysis comprises a confrontation with the Hauser-Feshbach theory, an investigation of the cross section distributions,

an autocorrelation analysis, and an estimation of the coherence width of the fluctuating component of the cross sections. In a further step a search for *correlated* structures in the excitation curves was undertaken by means of three frequently used statistical methods, namely the method of "counting maxima," the energy dependent deviation function, and the cross-correlation function.

II. EXPERIMENTAL PROCEDURE AND RESULTS

The measurements were performed at the tandem accelerator of the Eidgenössische Technische Hochschule (ETH), Zürich. A sputter type negative ion source attached to this accelerator provided both ^9Be and ^{12}C ions.⁸ Using in the experiment both combinations, i.e., a Be beam with a C target *and* a C beam with a Be target, it was possible to cover the whole angular region from 5° to 175° by performing measurements at angles in the forward hemisphere only, where the conditions given by the reaction kinematics are more favorable.

The beam was focused onto a target placed in the middle of a large 70 cm diameter scattering chamber. Self-supporting foils with a thickness of 40 or 60 $\mu\text{g}/\text{cm}^2$ were used as C or Be targets, respectively. The energy loss of the beam was equal to approximately 90 keV for the ^{12}C target and 250 keV for the ^9Be target. Special precautions were taken to keep the carbon deposit on the target during the measurements as small as possible. Thus the pressure in the scattering chamber was kept at less than 10^{-7} Torr and an 80 cm long piece of the beam line in front of the chamber was cooled with liquid nitrogen. Nevertheless, the contamination of the Be target with carbon deposits impeded or even prevented the analysis of some parts of the spectra at some angles. The influence of oxygen and other contaminations in the targets was practically insignificant.

The spectra of the light reaction products, i.e., protons, deuterons, tritons, and alpha particles, were detected simultaneously in four ΔE - E telescopes. Through a special multiplexer system, the pulses were transferred to a pair of analog-to-digital converters (ADC's) connected to a PDP-15 computer where an on-line analysis was performed. Si-semiconductor counters with thicknesses between 30 and 100 μm were used as ΔE counters, while 7 mm thick Li-drifted Si-counters served as E detectors. At small angles the entrance windows to the telescopes were covered by Al foils to prevent a

large overload of the counters by elastically scattered particles. The measurements were performed for the ^{12}C -target/ ^9Be -beam combination at the angles 5° , 10° , 14.7° , 20° , 24.7° , 30° , 44.7° , and 54.7° in the laboratory system, and for the reversed target/beam combination at the angles 5° , 10° , 20° , and 30° (lab). An angular resolution of the counter telescopes of approximately 1.5° was chosen in order to limit the kinematical energy spread and to obtain an overall resolution of the order of 250 keV.

The ^8Be ions emitted as reaction products were detected in three counter pairs measuring the alpha particles from the decay of ^8Be in coincidence.⁸ The detection angles were equal to 7.5° , 27.5° , and 47.5° (lab) using a ^9Be target and a ^{12}C beam.

The elastic scattering at backward angles was measured in four counter telescopes using a ^{12}C beam and detecting the recoiling ^9Be particles. In the two telescopes placed at extreme angles ionization chambers were used as ΔE detectors,⁹ while in the other two, thin semiconductor counters of a thickness below 10 μm were applied for this purpose. The scattering angles were 5° , 10° , 20° , and 30° (laboratory).

From the measured particle spectra the differential cross sections were determined for many states or unresolved groups of states of the residual nuclei. Table I gives a compilation of information on these states. The absolute normalization of the cross sections was obtained from a comparison with elastic scattering of ^9Be and ^{12}C , which on its part was normalized by observing the Rutherford scattering on a gold layer of known thickness evaporated on the target.¹⁰

Altogether 266 excitation curves were measured. Figure 1 and 2 show some examples. The error bars attached to the experimental points contain the statistical errors of the individual cross sections only and do not include the error of the normalization of the absolute values (3 to 5 % inaccuracies of the solid angles of the detectors and a 4% error in the determination of the ratio of gold to target atoms). In all cases quite a large energy dependence of the cross sections is visible. Besides a smooth, slowly varying component, rapidly fluctuating structures appear with a typical width of 0.5 MeV.

III. STATISTICAL ANALYSIS

In a search for intermediate resonances the experimental material should be submitted to a very careful statistical analysis with the aim of finding out to what extent the observed energy variations can be

TABLE I. Compilation of states of the residual nuclei observed in the measurements of excitation curves (excitation energies, spin, and parities).

${}^{20}\text{F}$:	0.0(2^+) 1.824(5^+), 1.873(2^-), 1.971(3^-), 2.044(2^+), 2.219(3^+)
${}^{19}\text{F}$:	0.0($\frac{1}{2}^+$), 0.109($\frac{1}{2}^-$), 0.197($\frac{5}{2}^+$) 1.346($\frac{5}{2}^-$), 1.459($\frac{3}{2}^-$), 1.554($\frac{3}{2}^+$) 2.780($\frac{9}{2}^+$) 3.907($\frac{3}{2}^+$), 3.999($\frac{7}{2}^-$), 4.033($\frac{9}{2}^-$) 4.378($\frac{7}{2}^+$), 4.555($\frac{5}{2}^+$), 4.557($\frac{3}{2}^-$), 4.648($\frac{13}{2}^+$), 4.683($\frac{5}{2}^-$) 5.106($\frac{5}{2}^-$), 5.337($\frac{1}{2}^+$), 5.425($\frac{7}{2}^-$), 5.465($\frac{7}{2}^+$), 5.500($\frac{3}{2}^+$), 5.54($\frac{5}{2}^+$), 5.62($\frac{3}{2}^-$)
${}^{18}\text{F}$:	0.0(1^+) 0.937(3^+), 1.042(0^+), 1.081(0^-), 1.121(5^+) 1.701(1^+) 2.101(2^-) 2.524(2^+) 3.060(2^+), 3.135(1^-), 3.357(3^+) 3.734(1^+), 3.787(3^-), 3.835(2^+) 4.119(3^+), 4.229(2^-), 4.361(1^+), 4.402(4^-) 4.650(4^+), 4.739(0^+), 4.849(1^-), 4.957(2^+)
${}^{17}\text{O}$:	0.0($\frac{5}{2}^+$) 0.871($\frac{1}{2}^+$) 3.055($\frac{1}{2}^-$) 3.841($\frac{5}{2}^-$)
${}^{13}\text{C}$:	0.0($\frac{1}{2}^-$) 3.086($\frac{1}{2}^+$) 3.68($\frac{3}{2}^-$), 3.85($\frac{5}{2}^+$)

described on the basis of the statistical reaction model. Since the fluctuating part of the cross section can be very similar in character to the expected resonances, the rapid variations of the cross section ought to be confronted with the predictions of a statistical fluctuation theory. However, the resonances could have similar widths to those of the fluctuations, and in addition, both structures might not differ significantly in magnitude (especially if resonances decay into many outgoing channels). Thus the analysis of the individual excitation curves should be supplemented by a correlation analysis extended to many reaction channels. Furthermore, *selected* subsets have to be considered since intermediate structures may be seen in certain reaction channels only.

A. Fluctuation analysis of individual excitation curves

Since the mean cross section varies slowly with energy due to a weak energy dependence of the compound nucleus or direct reaction mechanisms, this variation should be eliminated for the statistical analysis of fluctuations by means of a proper reduction of the experimental data. This is achieved by dividing the observed differential cross sections $\sigma(E)$ by a suitable mean value $\overline{\sigma(E)}$. Since the averaging procedure used to determine $\overline{\sigma(E)}$ can significantly influence the results, these effects were very carefully investigated prior to the analysis.

Three commonly used averaging procedures were tested: (1) simple moving averages over a suitable energy interval Δ , (2) repeated moving averages,¹¹

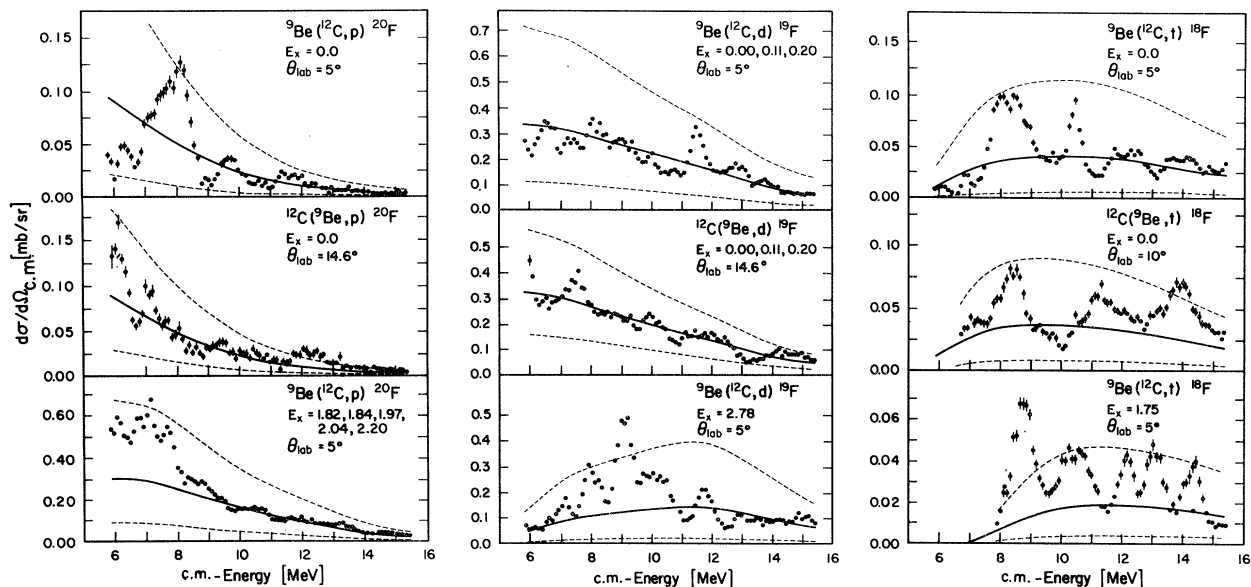


FIG. 1. Excitation curves for the emission of protons, deuterons, and tritons. Dots: experimental points; solid line: Hauser Feshbach theory prediction; dashed lines: 1% confidence limits for the fluctuations.

and (3) use of a polynomial or a spline function describing the mean cross section function. The first method leaves still quite large variations in the averaged excitation curve even if an averaging interval which is large compared to the widths of the fluctuations is used. The two other methods lead to

more smooth averaged curves; however, some systematic discrepancies appear, favoring too high or too low values of the averages in the regions of positive or negative curvatures of the mean curves, respectively.

As a result of these investigations,¹² the following

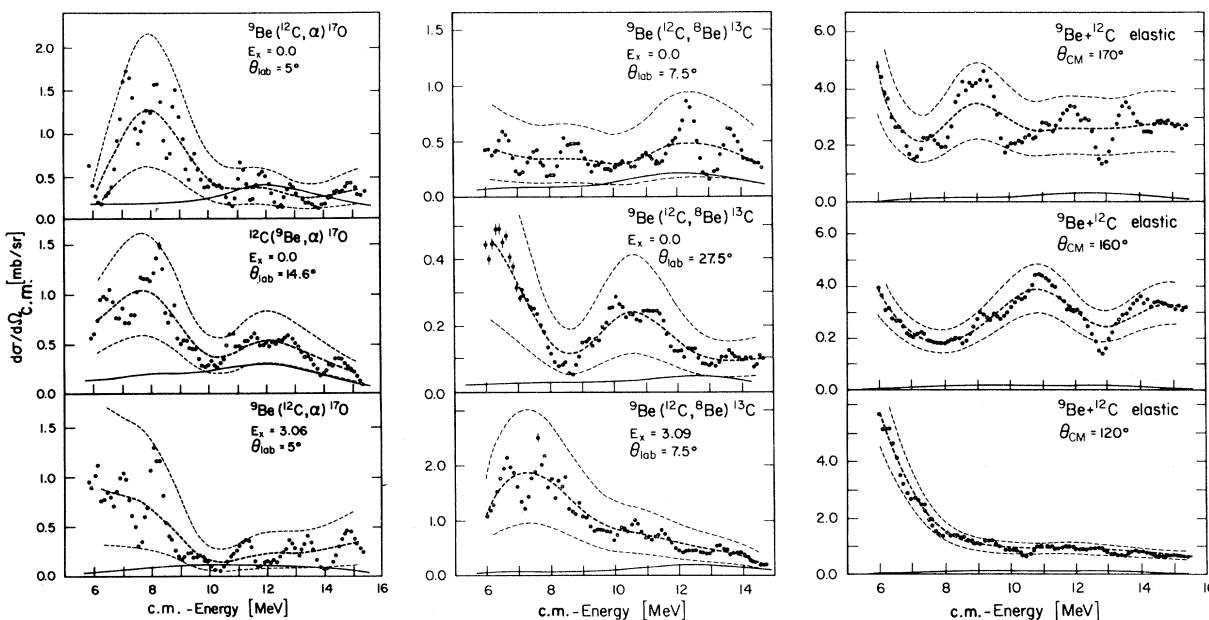


FIG. 2. Excitation curves for the emission of α particles, ^8Be ions, and for elastic scattering. Dots: experimental points; solid line: Hauser-Feshbach theory prediction; dark dashed line: averaged cross section; light dashed lines: 1% confidence limits for the fluctuations.

procedure based on method (2) was developed: Since the systematic deviations increase with the number of iterations, the general trend of the curves should be subtracted before averaging is repeated too often. This can, e.g., be done by subtracting, after a threefold application of moving averages, the obtained mean values from the original data points. The general behavior of the result is then relatively flat and the obtained points can be used as input to further averaging stages. This treatment of the data can be repeated after three further iterations. The mean cross sections are then, of course, obtained by adding the different correcting averages to the first mean function. With an averaging interval of $\Delta=1.8$ MeV chosen in this work, this method has the advantage of attaining a high degree of smoothing without affecting resonances too much and without biasing the mean cross sections. Periodic structures with half periods of 1.7 MeV or 900 keV are, e.g., reduced to 50% or 3%, respectively, while Breit-Wigner curves are damped to 44% for a full width Γ of 600 keV. Examples of such average excitation curves are shown as dark dashed lines in Fig. 2.

The energy averaged cross sections should be compared with the smooth part of the compound nucleus cross section. For this purpose the angular distributions of the evaporated light particles were measured at energies of 12, 14, 17, 20, 23.5, and 27 MeV (lab) and analyzed in terms of the Hauser-Feshbach model.¹³ A comparison of the theoretical predictions with the experimental data for proton, deuteron, and triton emission allowed us to determine the free parameters of the theory (cutoff angular momentum, level density parameters) and to calculate mean cross sections for all reaction channels including the compound elastic contribution for which a Moldauer factor¹⁴ of 2 was assumed.

The results are shown as solid lines in Figs. 1 and 2. For the proton and deuteron channels the calculated compound nucleus contributions follow the averaged measured excitation curves quite well. The differences do not exceed 20%. The agreement is not very good in the case of the triton channels, especially for the highest excited states of the residual nuclei. These discrepancies are most likely due to the inadequate knowledge of the optical potential for tritons and its energy dependence,¹⁵ which has to be used in the Hauser-Feshbach model calculation.

The compound nucleus contribution in the alpha particle, ${}^8\text{Be}$, and elastic channels is considerably lower than the average cross section extracted from

the present measurements. In all these channels there is a large direct reaction component.^{6,16,17} The average direct reaction contribution is determined as

$$d_k = \left\langle \frac{\bar{\sigma}_k - \sigma_k^{\text{HF}}}{\bar{\sigma}_k} \right\rangle, \quad (1)$$

where σ_k^{HF} is the calculated compound nucleus contribution in channel k , and $\langle \rangle$ denotes the average over the whole energy interval. The values of the d_k are approximately 50% in the alpha-particle channels and 75% and 90% in the ${}^8\text{Be}$ and elastic channels for the backward region covered by the present measurements.

The direct reaction contribution in the alpha particle and ${}^8\text{Be}$ channels has been estimated assuming that simple particle or cluster transfer processes are dominant. The DWBA or coupled-reaction-channel (CRC) model calculations reproduce quite well the energy dependence and magnitude of the average cross sections found in the present experiment.⁷ As the ${}^{12}\text{C}({}^9\text{Be},\alpha){}^{17}\text{O}$ reaction corresponds to a 5 nucleon transfer (in forward direction) or an 8 nucleon transfer (in backward direction) in these calculations, the possibility of a sequential transfer was also taken into account besides the simultaneous transfer of all nucleons. The contribution from the sequential transfer has a stronger energy dependence than that from the simultaneous transfer and is particularly significant in the region of lower energies.

The statistical properties of the fluctuating cross sections are characterized by the autocorrelation function defined as¹⁸

$$R_k(\epsilon) = \left\langle \left[\frac{\sigma_k(E+\epsilon)}{\sigma_k(E+\epsilon)} - 1 \right] \left[\frac{\sigma_k(E)}{\sigma_k(E)} - 1 \right] \right\rangle \\ = R_k(0) \cdot \frac{\Gamma^2}{\epsilon^2 + \Gamma^2}, \quad (2)$$

where Γ is the coherence width of the fluctuations. The value of $R_k(\epsilon)$ at $\epsilon=0$, i.e., the autocorrelation coefficient $R_k(0)$ is connected to the direct reaction contribution d_k and the number of effective channels n_k through the relation

$$R_k(0) = \frac{1 - d_k^2}{n_k}. \quad (3)$$

The n_k 's can be obtained from the Hauser-Feshbach cross sections according to a procedure proposed in Ref. 19. They depend only slightly on the energy so that all calculations could be performed with values

determined for 11.4 MeV (c.m.).

The results of the autocorrelation analysis depend on experimental factors such as the finite energy resolution, the total energy range, the step length in the measurements of the excitation curves, and especially on the applied averaging procedure. The influences of these conditions were investigated by many authors,^{20–23} and correction factors K_R and K_Γ have been proposed which should be applied to the quantities extracted directly from the analysis: $R_k^{\text{corr}}(0) = K_R R_k^{\text{obs}}(0)$ and $\Gamma = K_\Gamma \Gamma^{\text{obs}}$. For the energy averaging interval of 1.8 MeV (17 experimental points), used throughout this analysis, the correction factors have values $K_R = 2.5 \pm 0.4$ and $K_\Gamma = 2.2 \pm 0.3$. The errors ascribed to these values take into account the spread of values proposed by different authors as well as the slight dependence on d_k and n_k in the range of interest. Averaging effects contribute roughly 80% to these values for the correction factors and effects of the finite range of experimental data 20%, while the influence of the energy resolution was negligible.

Examples of autocorrelation functions obtained in this analysis are shown in Fig. 3. For large values of ϵ the function oscillates around zero due to effects connected to the limited range of data. The root mean square (rms) value of these oscillations is in good agreement with the prediction of the theory of fluctuations,²⁰ i.e., with $\sqrt{\pi \cdot \Gamma^{\text{obs}} / \sqrt{2 \cdot (E_2 - E_1)}}$. The corrected values of the autocorrelation coefficients extracted from the experimental excitation curves (R^{corr}) are compatible with those calculated from formula (3) using d_k and n_k from the Hauser-Feshbach analysis. The ratios $R^{\text{corr}}/R^{\text{HF}}$ scatter considerably. Nevertheless, the *mean* value for the curves of data set *A* (Table II), e.g., is 1.06 ± 0.09 for an averaging interval Δ of 1.8

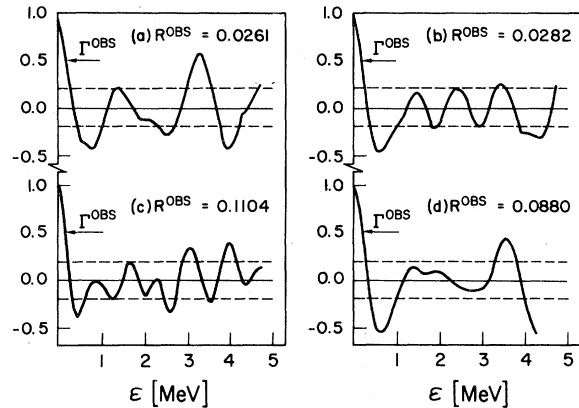


FIG. 3. Examples of normalized autocorrelation functions for the excitation curves: (a) $^{12}\text{C}(^9\text{Be},p)^{20}\text{F}$, $E_x = 1.82$ to 2.20 MeV, $\theta_{\text{lab}} = 10^\circ$; (b) $^9\text{Be}(^{12}\text{C},d)^{19}\text{F}$, $E_x = 0.0, 0.11, 0.20$ MeV, $\theta_{\text{lab}} = 5^\circ$; (c) $^9\text{Be}(^{12}\text{C},\alpha)^{17}\text{O}$, $E_x = 0.0$, $\theta_{\text{lab}} = 5^\circ$; (d) $^9\text{Be}(^{12}\text{C},^8\text{Be})^{13}\text{C}$, $E_x = 0.0$, $\theta_{\text{lab}} = 7.5^\circ$. The dashed lines give the standard deviation of $R(\epsilon)$ from zero at large values of ϵ due to the finite range of experimental data.

MeV, 1.13 ± 0.12 for $\Delta = 3.3$ MeV, and it is also close to 1 for other subsets.

The values of the coherence width obtained from this analysis Γ^{obs} are shown in Fig. 4 as a function of the averaging interval. After correcting for the finite averaging interval, a mean coherence width

$$\Gamma = \frac{1}{N} \sum_{i=1}^N K_\Gamma \cdot \Gamma_i^{\text{obs}} = 470 \pm 90 \text{ keV}$$

can be extracted from the observed value Γ^{obs} for the different reaction channels. In Fig. 4 the dashed lines represent the expected values for the observed coherence width Γ/K_Γ using a Γ of 470

TABLE II. Composition of the data sets for the correlation analyses.

Set	Total	p	Number of exc. curves				
			d	t	α	^8Be	Elastic
<i>A</i>	58	10	19	2	19	6	2
<i>B</i>	34	6	10	2	12	3	1
<i>C</i>	20	4	6	1	8		1
Protons		10					
Deuterons			19				
Tritons				14			
Alphas					19		
^8Be						6	
Elastic + ^8Be						6	3

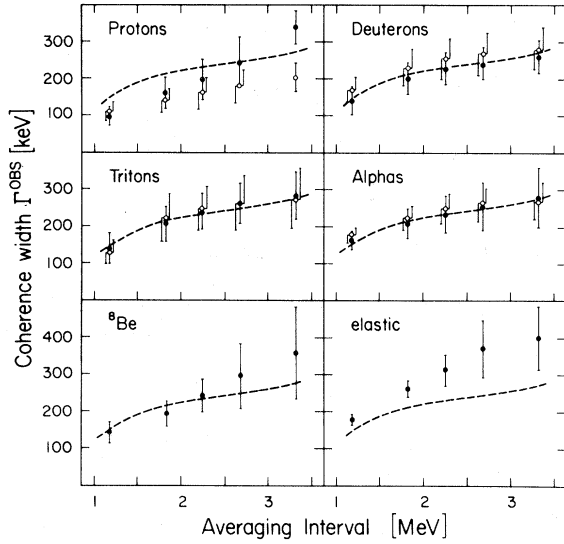


FIG. 4. Values for the coherence widths Γ^{obs} obtained directly from the excitation curves for emission of p , d , t , α , ${}^9\text{Be}$, and for elastic scattering as a function of the averaging interval, calculated for the forward (open circles) and the backward direction (full points). The dashed lines show the expected variations of the observed coherence widths due to the averaging interval dependence of the correction factor K_Γ .

keV and taking into account the dependence of K_Γ on the averaging interval which follows from Refs. 20–23. For light particles, i.e., p , d , t , and α , the averaging interval dependence is compatible with the expected slope of the correction factor, K_Γ . With the exception of the proton data for very large averaging intervals, $\Delta > 2.5$ MeV, measurements in the forward and backward hemisphere give also identical results. A more pronounced dependence on the averaging interval appears in the ${}^9\text{Be}$ and elastic channels, a fact which could be a consequence of a larger direct reaction contribution in these channels.

Information on the coherence width of fluctuations can be obtained in an independent way from counting maxima.¹⁸ The coherence width is calculated from the number of maxima k per energy unit in the excitation functions according to the formula

$$\Gamma = b \frac{0.55}{k},$$

where b is a correction factor taking into account effects of nonideal experimental conditions such as the finite energy steps at which the points in the excitation curve have been measured. The number of counted maxima depends to some extent on the cri-

terion assumed for their identification. In our analysis the i th data point of the curve was interpreted as a maximum when two neighboring points on each side are lower, i.e., when $\sigma(E_i) > \sigma(E_{i-2})$, $\sigma(E_{i-1})$, $\sigma(E_{i+1})$, and $\sigma(E_{i+2})$. The number of maxima estimated by this method is independent of any averaging procedure and agrees well with that obtained simply by counting according to a judgment by the eye. In the experimental excitation curves $k = 1.18 \pm 0.25$ maxima/MeV are observed. With a correction factor $b = 1.0 \pm 0.1$ from Refs. 21 and 22 we obtain the value

$$\Gamma = 470 \pm 110 \text{ keV},$$

in agreement with that obtained in the autocorrelation analysis. The values of the coherence width determined from the experimental excitation curves are rather high, but not in disagreement with systematic compilations of their dependence on A and excitation energy. A compilation of Shapira *et al.*²³ delivers values between 150 and 300 keV for the excitation energies under consideration, while Eberhard and Richter²⁴ give values of 200 to 400 keV at an excitation energy corresponding to the lower end of the present investigations.

A comparison of the distribution of the measured cross sections with the theoretical predictions given in the statistical model by the formula²⁵

$$P(y_k) = \left[\frac{n_k}{1-d_k} \right]^{n_k} \cdot y_k^{n_k-1} \cdot \exp \left[-n_k \frac{y_k + d_k}{1-d_k} \right] \times \frac{I_{n_k-1} [2n_k \sqrt{y_k d_k} / (1-d_k)]}{[n_k \sqrt{y_k d_k} / (1-d_k)]^{n_k-1}} \quad (4)$$

can serve as a further test of the statistical nature of the observed structures in the excitation curves. Here $y_k = \sigma_k / \bar{\sigma}_k$ is the reduced cross section in the channel k and I_μ denotes the modified Bessel function of order μ . In Fig. 5 examples of histograms of experimental cross section distributions are shown for different exit channels. The theoretical distributions were determined from formula (4) using average values for the direct reaction contribution $d_k = \langle 1 - \sigma_k^{\text{HF}} / \bar{\sigma}_k \rangle$ (set equal to zero for the proton, deuteron, and triton channels) and for the number of effective channels n_k calculated at an energy of 11.4 MeV (c.m.). Several nonideal experimental conditions, and mainly the effect of the averaging procedure, tend to reduce the variance of the experimental distribution. These effects, discussed for the autocorrelation function, were taken into account by replacing n_k in the distribution

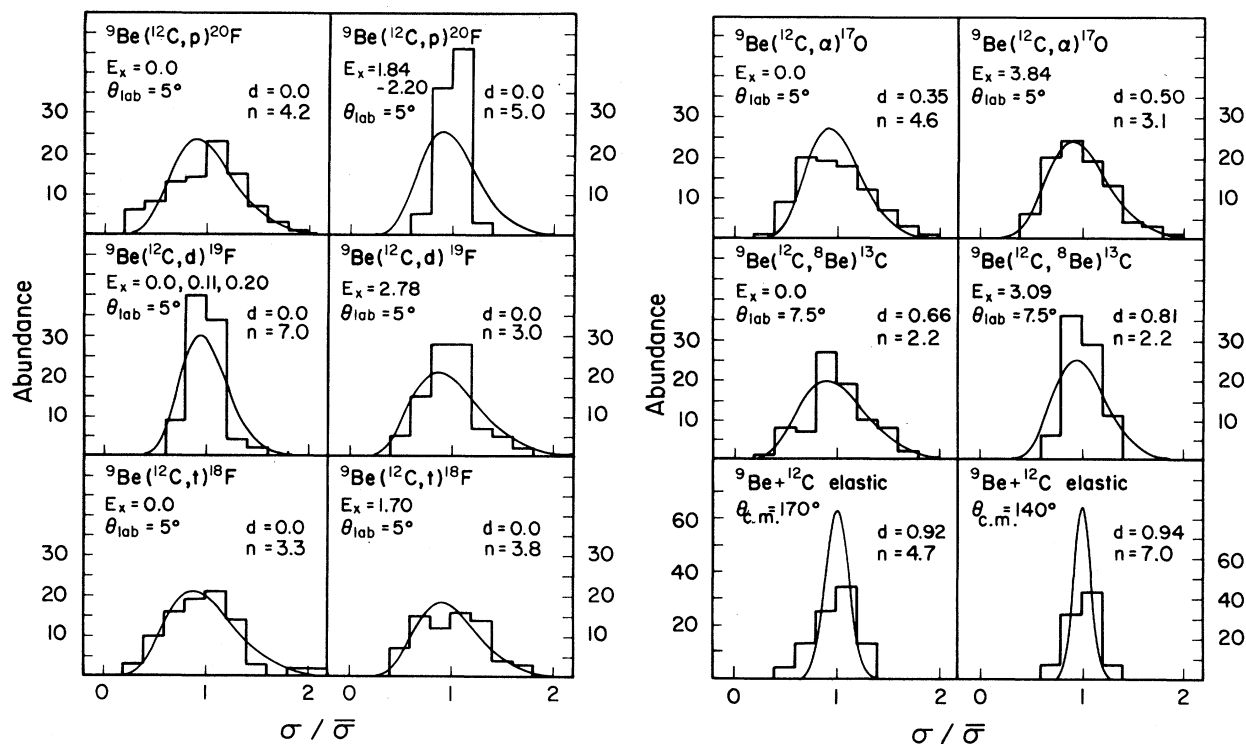


FIG. 5. Histograms of the probability distributions of cross sections for various reaction channels. The smooth curves show the statistical model predictions calculated for a number of effective channels n and a direct reaction contribution d .

$P(y_k)$ of the cross sections [expression (4)] by n_k times the correction factor K_R . This causes a reduction of the variance of the theoretical distribution,

$$s^2 = R(\epsilon=0) = (1 - d_k^2) / n_k,$$

by a factor K_R .

For localizing possible nonstatistical structures in energy 1% probability confidence limits were drawn as light dashed lines in Figs. 1 and 2. These confidence limits were calculated using the distribution function $P(y_k)$. Hauser-Feshbach compound nucleus cross sections were taken as mean cross sections for the proton, deuteron, and triton channels. For the other channels values determined by the modified running average procedure could be used as mean values. Consequently, $n_k \cdot K_R$ had to be inserted in the formulas for calculating the fractiles instead of n_k in the latter cases. It should be pointed out that the absolute width of the fluctuation band corresponding to the 1% confidence level is also large in channels where the compound nucleus contribution is small, provided the number of effective channels n_k is small.

This analysis of the individual excitation curves

shows that the structures appearing there are essentially consistent with predictions of the statistical reaction model. In a representative selection of excitation curves (set A in Table II) 0.8% of the cross sections lie above and 1.6% below the 1% confidence limits for fluctuations around the mean cross sections, which corresponds well to the expected number.

B. Correlation analysis

Since intermediate states decay in general into many reaction channels, their effects observed in a single channel can be damped significantly. Therefore, the statistical analysis of individual excitation curves has to be supplemented by a correlation analysis. In such an analysis the statistical independence between the compound nucleus components of the excitation curves under investigation is assumed. In order to avoid trivial angular correlations, pairs of such curves (i, j) for the transition to the same final state were included in the same data set only if they were measured at angles outside the relevant coherence angle $|\theta_i - \theta_j| > \theta_{\text{coh}}$. Following the discussion in Ref. 26, the value of the black

nucleus approximation, i.e., $\theta \sim 6^\circ - 9^\circ$ is too small. Therefore, a bigger value of about 30° (c.m.) was assumed.

Table II presents a compilation on the composition of the data sets used in the correlation analysis. The sets *A*, *B*, and *C* include different curves for all reaction channels (*p*, *d*, *t*, α , ${}^8\text{Be}$, elastic scattering) corresponding to transitions to various states of residual nuclei. Within one set the differences between the emission angles are greater than 30° (c.m.) for two curves belonging to the same final state. The inclusion of reaction channels with the same final partition but for different angles is always a compromise between avoiding correlations and increasing the number of data. With the exception of the triton channels all sets corresponding to one particular reaction product were selected as subsets of set *A*. Only excitation curves which cover a consecutive energy range not smaller than 9 MeV (7.5 MeV for the triton subset) are taken into account in the correlation analysis. Owing to limitations forced by reaction thresholds and target contaminations, this condition reduced the number of analyzed curves by a factor of 2 as compared with the total experimental material.

Three statistical tests commonly in use²⁷ were applied in our analysis for searching for correlated structures in the excitation curves:

(2) *Method of counting the maxima.* This very simple method consists of counting at each energy the number of peaks in all excitation curves.²⁷ In this case, the probability distribution of the number of maxima is known and simply given by a binomial distribution

$$P(k) = \binom{N}{k} p^k (1-p)^{N-k} \quad (5)$$

P is the probability for finding in a set of *N* curves at a given energy *k* (correlated) maxima; *p*, the probability for each point to be a maximum, is derived from the total number of maxima divided by the total number of measured points. The knowledge of the probability distribution allows us to ascribe confidence levels to the results obtained by this procedure.

Results of this method (using the criterion of identifying a maximum given in Sec. IIA) are presented in Fig. 6. In order to take into account possible small energy shifts of correlated structures in different excitation curves, the number of curves in which a maximum occurs in a specific point or in two neighboring points are added. In formula (5), *p* then has to be multiplied by a factor of 3.

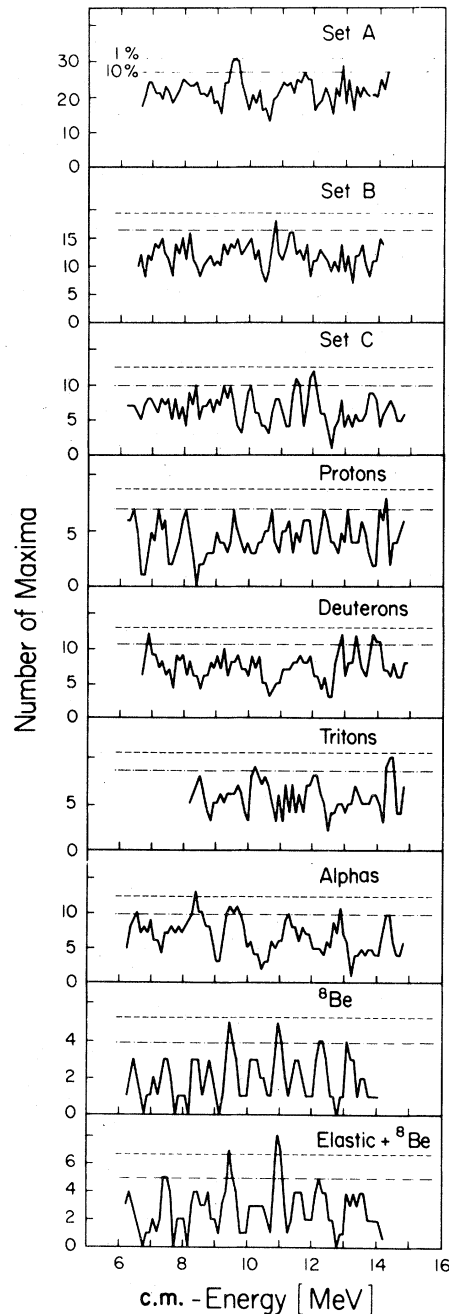


FIG. 6. Numbers of maxima for different data sets. The 1% and the 10% confidence limits, calculated from the binomial distribution, are shown as the dashed and dotted-and-dashed lines, respectively.

The dotted-and-dashed lines in Fig. 6 show the 1% and 10% confidence limits calculated from the binomial distribution, respectively.

Besides statistical independence, the validity of formula (5) assumes that the number of maxima per

unit energy interval is constant in the whole investigated energy range and is independent of the reaction channel. The correctness of the first assumption follows from the horizontal shape of the averaged test functions in Fig. 6. In order to check the second hypothesis the number of maxima per excitation function is plotted in Fig. 7 for the curves of set *A* as well as for two subsets. The mean number of maxima is the same in all three cases and also the widths of the distributions are compatible with theoretical predictions.

In Fig. 6 no indication of statistically significant correlated structures can be seen. An accumulation of maxima resulting in peaks reaching the 1% limit for set *A* at 9.5 MeV, for the α -particle subset at 8.3 MeV, and for the ^8Be and elastic channel subsets at 9.4 and 11.0 MeV is still compatible with a statistically acceptable expectation.

(2) *Energy dependent deviation function.* This widely used test function for the localization of

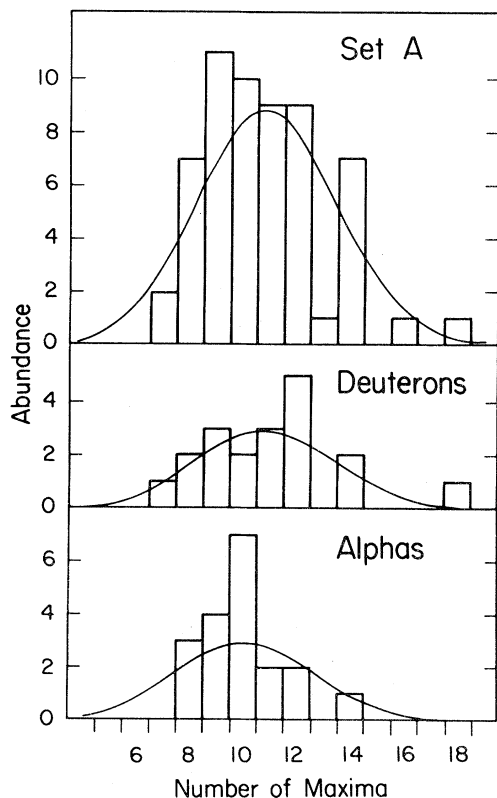


FIG. 7. Distribution of the number of maxima per excitation curve for data set *A* and for the deuteron and α -particle subsets. The smooth curves show the binomial distributions.

correlated structures is defined by the expression

$$D(E) = \frac{1}{N} \sum_{i=1}^N \left[\frac{\sigma_i(E)}{\overline{\sigma_i(E)}} - 1 \right], \quad (6)$$

where $\sigma_i(E)$ is the measured cross section at a fixed angle for one final state, $\overline{\sigma_i(E)}$ denotes its energy averaged value, and the sum extends over N statistically independent excitation curves.

Recently a procedure was developed which allows us to calculate the probability distribution function for the deviations, $P(D)$.²⁸ Assuming uncorrelated excitation curves, the characteristic function of $P(D)$ can be calculated easily as a product of the characteristic functions of the original distributions [Eq. (4)]. For an exact specification of the 1% confidence limits the Fourier transform necessary to find $P(D)$ has to be done numerically, but the probability density of $(D+1)$ is approximately the same as that of the cross sections [Eq. (4)], replacing n_k by $n_{\text{tot}} = \sum n_k$ and d_k by $\langle d_k \rangle$.

In Fig. 8 the abundance distribution of the deviations for set *A* is compared with that following from the theory. No accumulation of events in the tails of the distribution which could indicate the presence of marked nonstatistical components in the fluctuating part of the cross section is seen. On the other hand, however, Table III shows that the variance s^2 of the observed deviations is rather high

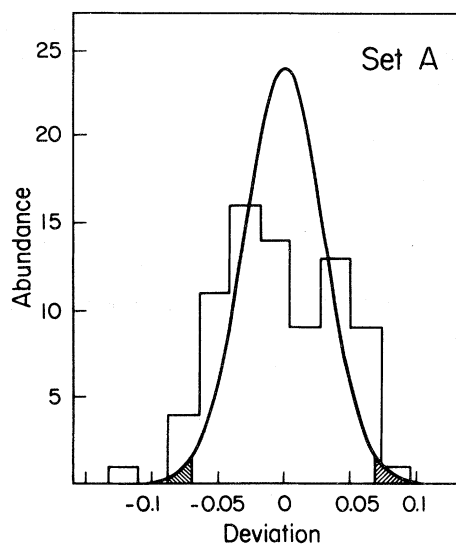


FIG. 8. Histogram of the probability distribution of the deviations calculated from the experimental excitation curves of data set *A*. The smooth line shows the theoretical distribution, the shaded areas denote the regions corresponding to the 1% confidence levels.

TABLE III. Comparison of the observed standard deviation s^{obs} of the deviations with values calculated from the observed autocorrelation coefficient $s(R^{\text{obs}})$ and from the Hauser-Feshbach analysis $s(R_{\text{HF}}^{\text{corr}})$ using formula (7).

	$s(R^{\text{obs}})$	$s(R_{\text{HF}}^{\text{corr}})$	s^{obs}
Set A	0.030	0.029	0.044
Protons	0.067	0.068	0.074
Deuterons	0.031	0.039	0.041
Alphas	0.070	0.064	0.112
Elastic + ${}^8\text{Be}$	0.063	0.067	0.082

compared with values following from the formulas

$$s = \frac{1}{N} \sqrt{\sum R_k^{\text{obs}}(\epsilon=0)}$$

or

$$s = \frac{1}{N} \sqrt{\sum \frac{1-d_k^2}{n_k} \cdot \frac{1}{K_R}} \quad (7)$$

This, and the fact that the experimental distribution shows a double-peaked structure (cf. Fig. 8), is an indication that there is some nonstatistical contribution to the excitation curves. Since the deviations depend to some extent on the averaging method, such a behavior could be produced by inadequacies of this procedure. Furthermore, the measurements taken at different angles for a given final state are in fact not completely uncorrelated (cf. the remarks at the beginning of this section), which could also increase the variance of the deviations.

The detailed results of the deviation analysis are presented in Fig. 9, in which the experimental deviation functions and the upper (f_u) and lower (f_l) fractiles corresponding to the 1% confidence levels are shown. In these calculations the damping of the fluctuations due to the averaging procedure is taken into account again by replacing in all formulas the number of effective channels n_k by the product of n_k and the correction factor K_R . Owing to uncertainties in the number of effective channels and in the direct reaction contributions, the fractiles are determined with an accuracy of approximately 20%.

Some similarity seen in the deviation function for the sets A, B, and to some extent, also C, containing curves for the same partitions but different angles, had to be expected since different sets contain curves lying within the coherence angle.

In the deviation function for set A and for α par-

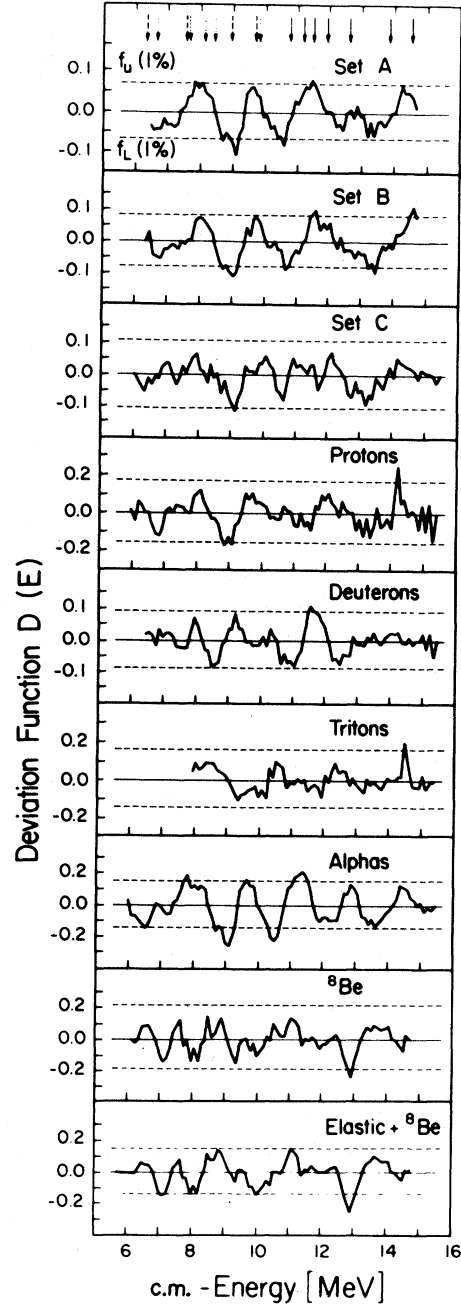


FIG. 9. Deviation functions for different sets of experimental data. The dashed lines show the fractiles corresponding to the 1% confidence levels. The arrows in the upper part of the diagram indicate energies at which other authors (Refs. 2, 4, and 5) claimed to see resonances.

ticles, two especially deep minima exceeding the 1% confidence limit are visible at the energies 9 and 10.5 MeV. The maximum appearing between them corresponds to the energy 9.64 MeV at which other

authors⁵ are inclined to identify a resonance. This maximum is also persistent when the averaging interval is changed. The deviation functions for protons, deuterons, and tritons give no clear hint of possible correlations. For alpha particles the structure of the deviation function is more pronounced. Some of the maxima reach the 1% significance limit and have a periodic, regular character. For the ⁸Be channel the general character of the deviations is in agreement with the statistical theory. Combining ⁸Be and elastic scattering data in one data set changes the shape of the deviation function only slightly, indicating some correlation between these two channels. This could, e.g., be due to a considerable coupling between them as a consequence of the strong direct reaction contribution in both channels.²⁹

The consistency between the results of the correlation analysis performed with the method of counting maxima and that deduced from the deviation function can be judged by comparing Figs. 6 and 9. In the points where the number of correlated maxima is larger or smaller than the average value, the deviation function also shows a maximum or minimum, respectively.

(3) *Cross correlation coefficients and functions.* The cross correlation coefficients calculated for pairs of channels i and k according to the formula

$$C_{ik} = \frac{\left\langle \left[\frac{\sigma_i(E)}{\sigma_i(E)} - 1 \right] \left[\frac{\sigma_k(E)}{\sigma_k(E)} - 1 \right] \right\rangle}{R_i(\epsilon=0)^{1/2} R_k(\epsilon=0)^{1/2}} \quad (8)$$

sheds light on the problem of stronger coupling or correlations between specific reaction channels. For uncorrelated curves a coefficient close to zero is expected. Figure 10 shows results of such an analysis performed for set A . The experimental distribution of the C_{ik} 's is symmetric around a mean value of 0.003. Not only the average value but also the width of the obtained distribution is in excellent agreement with the assumption of a lack of any correlation between the curves. The finite width of the distribution results from the finite range $E_2 - E_1$ of the energy interval under investigation and from the averaging of the data.

The standard deviation, $s = 0.20$, is in agreement with the expected value of the distributions, $s = \sqrt{\pi \cdot \Gamma^{\text{obs}} / 2 \cdot (E_2 - E_1)}$,²⁰ giving in our case 0.19. In Fig. 10 the normal distribution with this variance is also drawn. From this large variance it follows that between some measured curves a considerable similarity in shape has to be expected for pure-

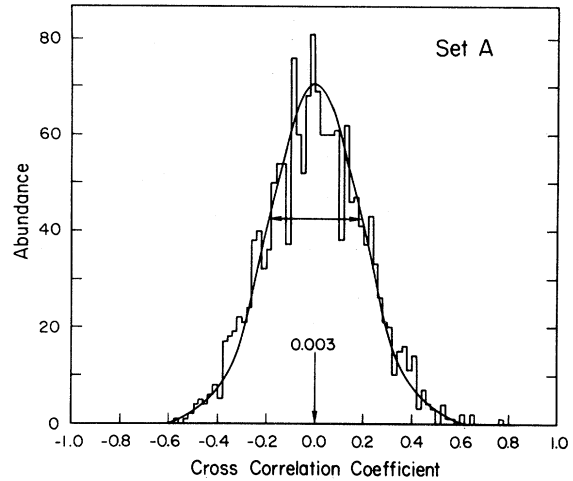


FIG. 10. Distribution of the cross-correlation coefficients C_{ik} for set A . The smooth line shows the normal distribution with the mean value 0 and a variance corresponding to the finite range of the measurements (see text).

ly statistical reasons. A detailed inspection of the data reveals that the highest values for the coefficient C_{ik} are obtained for pairs of curves corresponding to the same final state but measured at neighboring angles included in the set. This fact indicates that the value of the coherence angle [30° (c.m.)] was rather underestimated.

Similarly as the deviation function or counting the maxima, the cross correlation function

$$C(E) = \frac{2}{N(N-1)} \sum_{i < k} \frac{\left[\frac{\sigma_i(E)}{\sigma_i(E)} - 1 \right] \left[\frac{\sigma_k(E)}{\sigma_k(E)} - 1 \right]}{R_i(\epsilon=0)^{1/2} R_k(\epsilon=0)^{1/2}} \quad (9)$$

can be used for localizing correlated structures. The sum extends over all pairs of excitation curves within a given data set. Since the terms in the sum are not statistically independent, the simple method of multiplying characteristic functions to calculate $P(C)$ is not applicable in this case. No procedure to ascribe confidence levels to observed structures seems to be known up to now.

The cross correlation functions determined for set A and several subsets are presented in Fig. 11. Sharp peaks coincide with maxima and minima in the deviation function.

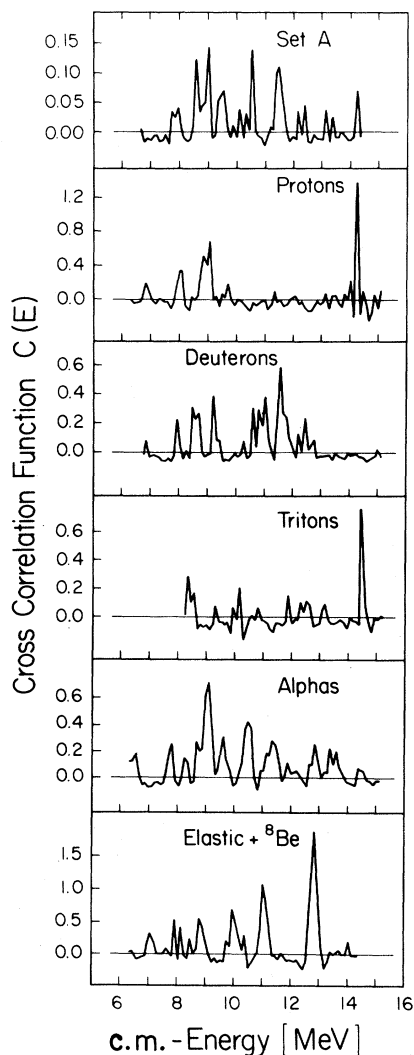


FIG. 11. Cross-correlation functions for different data sets.

IV. SUMMARY AND DISCUSSION OF RESULTS

On the basis of the large sample of experimental material comprising more than 250 excitation curves for the emission of protons, deuterons, tritons, α particles, ${}^8\text{Be}$ ions, and for elastic scattering in the energy range from 5.9 to 15.4 MeV, the system ${}^9\text{Be} + {}^{12}\text{C}$ was extensively analyzed with the aim of localizing possible nonstatistical structures and discriminating them from the background of statistical fluctuations.

The Hauser-Feshbach compound nucleus cross section describes well the average cross sections for the emission of protons, deuterons, and tritons. It is considerably smaller in the α particle, ${}^8\text{Be}$, and elastic scattering channels, indicating a large contribution from direct reactions.

The performed statistical model analysis shows a good agreement of the structures appearing in the excitation curves with the predictions of the model. A comparison of the distribution of the reduced cross sections in the individual reaction channels with the theoretical distribution gives no indication of any nonstatistical anomalies. The maxima in the single curves reach the 1% confidence level only in a few cases. Also the analysis of the autocorrelation functions indicates clearly the statistical origin of the observed oscillations in the excitation curves. The values of the experimental autocorrelation coefficients, corrected for the averaging interval and the finite range of data, agree with the statistical model prediction. The coherence widths extracted from the autocorrelation curves and those obtained by the method of counting the maxima are in agreement and have values not significantly different from those following from systematics of the A and energy dependence.

The correlation analysis performed by means of counting correlated maxima, by means of the energy dependent deviation function, as well as the correlation function does not prove the existence of any marked correlated structures. The number of peaks in these energy dependent curves reaching the 1% significance level is not inconsistent with the statistical expectation.

In conclusion, it can be stated that, taking into consideration the excitation curves only, no definite conclusion can be drawn concerning the existence of possible resonances in the ${}^9\text{Be} + {}^{12}\text{C}$ system in the energy region under consideration. As a resonance might possibly be spread over many channels and therefore not be found through an analysis of the excitation curves, some other method should be applied which is sensitive to other effects connected with resonances. In the case of systems with channel spin 0 and a small contribution from direct reaction processes, such a possibility is given by the analysis of angular distributions. However, in the system under consideration the situation is quite unfavorable for such an analysis, since the channel spin is different from zero. Furthermore, if we consider the α particle or ${}^8\text{Be}$ channels, where one could assume most likely an influence of some resonances, the dominating direct reaction contribution,

favoring partial waves in a limited region, certainly obscures the situation. According to the performed analysis of the cross sections, resonances—if any—can manifest themselves by a *small* increase of cross sections only. There is little chance to trace them by observation of the angular distributions in the presence of a strong background from direct processes.

ACKNOWLEDGMENTS

The authors gratefully acknowledge the financial support of the Swiss National Science Foundation. Special thanks are due to Professor K. Grotowski and the staff of the Nuclear Detector Laboratory of the Jagellonian University for providing the thick semiconductor detectors used in the experiment.

-
- *On leave from the Institute of Physics, Jagellonian University, Cracow, Poland.
- ¹D. L. Hanson, R. G. Stokstad, K. A. Erb, C. Olmer, M. W. Sachs, and D. A. Bromley, *Phys. Rev. C* **9**, 1760 (1974).
- ²J. F. Mateja, A. D. Frawley, A. Roy, J. R. Hurd, and N. R. Fletcher, *Phys. Rev. C* **18**, 2622 (1978).
- ³K. Bodek, M. Hugi, J. Lang, R. Müller, E. Ungricht, L. Jarczyk, B. Kamys, and A. Strzałkowski, *Phys. Lett.* **82B**, 369 (1979).
- ⁴X. Aslanoglou, G. Vourvopoulos, D. Pocanic, and E. Holub, in *Proceedings of the International Conference on Resonance Behavior of Heavy Ion Systems, Aegean Sea—1980*, edited by G. Vourvopoulos (Nuclear Research Center "Democritos," Athens, 1981).
- ⁵L. C. Dennis, K. R. Cordell, R. R. Doering, R. L. Parks, S. T. Thornton, J. L. C. Ford, Jr., J. Gomez del Campo, and D. Shapira, *Nucl. Phys.* **A357**, 521 (1981).
- ⁶L. Jarczyk, B. Kamys, J. Okołowicz, J. Sromicki, A. Strzałkowski, H. Witała, Z. Wróbel, M. Hugi, J. Lang, R. Müller, and E. Ungricht, *Nucl. Phys.* **A325**, 510 (1979).
- ⁷H. Witała, thesis, Jagellonian University, Cracow, 1981.
- ⁸J. Unternährer, thesis, Eidg. Tech. Hochsch. (Zürich), No. 5947 (1977).
- ⁹E. Ungricht, thesis, Eidg. Tech. Hochsch. (Zürich), No. 6500 (1979).
- ¹⁰E. Ungricht, D. Balzer, M. Hugi, J. Lang, R. Müller, L. Jarczyk, B. Kamys, and A. Strzałkowski, *Nucl. Phys.* **A313**, 376 (1979).
- ¹¹G. U. Yule and M. G. Kendall, *An Introduction to the Theory of Statistics* (Griffin, London, 1964).
- ¹²M. Hugi, thesis, Eidg. Tech. Hochsch. (Zürich), No. 6865 (1981).
- ¹³L. Jarczyk, B. Kamys, A. Magiera, J. Sromicki, A. Strzałkowski, G. Willim, Z. Wróbel, D. Balzer, K. Bodek, M. Hugi, J. Lang, R. Müller, and E. Ungricht, *Nucl. Phys.* **A369**, 191 (1981).
- ¹⁴P. A. Moldauer, *Phys. Rev. C* **11**, 426 (1975).
- ¹⁵C. M. Perey and F. G. Perey, *At. Data Nucl. Data Tables* **17**, 1 (1976).
- ¹⁶L. Jarczyk, B. Kamys, A. Strzałkowski, M. Hugi, J. Lang, R. Müller, and E. Ungricht, *J. Phys. G* **5**, 565 (1979).
- ¹⁷L. Jarczyk, J. Okołowicz, A. Strzałkowski, K. Bodek, M. Hugi, J. Lang, R. Müller, and E. Ungricht, *Nucl. Phys.* **A316**, 139 (1979).
- ¹⁸D. M. Brink and R. O. Stephen, *Phys. Lett.* **5**, 77 (1963).
- ¹⁹R. A. Dayras, R. G. Stokstad, Z. E. Switkowski, and R. M. Wieland, *Nucl. Phys.* **A265**, 153 (1976).
- ²⁰P. J. Dallimore and I. Hall, *Nucl. Phys.* **88**, 193 (1966).
- ²¹A. Van der Woude, *Nucl. Phys.* **80**, 14 (1966).
- ²²J. D. A. Roeders, thesis, University of Groningen, 1971.
- ²³D. Shapira, R. G. Stokstad, and D. A. Bromley, *Phys. Rev. C* **10**, 1063 (1974).
- ²⁴K. A. Eberhard and A. Richter, in *Statistical Properties of Nuclei*, edited by J. B. Garg (Plenum, New York, 1972), p. 139.
- ²⁵T. Mayer-Kuckuk, in *Proceedings of the Summer Meeting of Nuclear Physicists*, edited by N. Cindro (Federal Nuclear Commission of Yugoslavia, 1964), p. 167.
- ²⁶P. Braun-Munzinger and J. Barrette, *Phys. Rev. Lett.* **44**, 719 (1980).
- ²⁷L. C. Dennis, T. S. Thornton, and K. R. Cordell, *Phys. Rev. C* **19**, 777 (1979).
- ²⁸J. Lang, M. Hugi, R. Müller, J. Sromicki, E. Ungricht, H. Witała, L. Jarczyk, and A. Strzałkowski, *Phys. Lett.* **104B**, 369 (1981).
- ²⁹C. A. Engelbrecht and H. A. Weidenmüller, *Phys. Rev. C* **8**, 859 (1973).